Research Square

Preprints are preliminary reports that have not undergone peer review.
They should not be considered conclusive, used to inform clinical practice,
or referenced by the media as validated information.

ANOMALOUS NONEQUILIBRIUM EFFECTS IN SUPERSONIC RAREFIED FLOW

Vladimir Aristov

aristovvl@yandex.ru

Federal Research Center “Computer Science and Control” of the Russian Academy of Sciences

Timur Mordukhay

Khristianovich Institute of Theoretical and Applied Mechanics of the Siberian Branch of Russian Academy of Sciences

Sergei Novopashin

Novosibirsk State University

Research Article

Keywords:

Posted Date: November 24th, 2026

DOI: https://doi.org/10.21203/rs.3.rs-11700694/v1

License: This work is licensed under a Creative Commons Attribution 4.0 International License.
Read Full License

Additional Declarations: No competing interests reported.

ANOMALOUS NONEQUILIBRIUM EFFECTS IN SUPERSONIC RAREFIED FLOWS

VV. Aristov[1], T.A. Mordukhay[2], S.A. Novopashin[3]

[1]Federal Research Center "Computer Science and Control" of Russian Academy of Sciences
[2]Khristianovich Institute of Theoretical and Applied Mechanics of the Siberian Branch of Russian Academy of Sciences
[3]Novosibirsk State University

e-mail: aristovvl@yandex.ru

ABSTRACT

This study investigates nonequilibrium rarefied gas flows that exhibit novel and diverse nonclassical effects of interest from several perspectives. A series of direct Monte Carlo simulations confirms our previous results for a monatomic gas obtained with the direct method for solving the Boltzmann equation. For a diatomic gas (N_2), the DSMC approach is implemented using the SMILE++ software system. The analysis is performed in a two-dimensional plane formulation. It is shown that the Fourier law is violated in the nonequilibrium supersonic flow behind a grid. Calculations of the fields of translational, rotational, and overall temperature are presented, and the results demonstrate anomalous transport downstream. These effects are also the subject of an experimental investigation using the electron beam technique, and the numerical solutions are compared with the experimental results. The latter confirm the predicted behavior of nonequilibrium rotational states downstream of the grid. A comparison of the rotational-level populations in the calculations and in the experiment demonstrates good qualitative agreement. Some possible application perspectives for cooling microchips using the anomalous heat transfer effect are also discussed.

Key words: Nonequilibrium flows - Boltzmann equation - Anomalous transport - Experiment

1 Introduction

The study of highly nonequilibrium gas flows is gaining considerable importance (Akhlaghi et al. 2023; Schafer et al. 2025): new effects in nonequilibrium gas flows are of interest from both theoretical and practical points of view. For example, thermal transpiration is used in various models of Knudsen pumps, and thermophoresis can now be applied through macroscopic membranes to study atmospheric layers. Some calculations based on the direct method (Unified Flow Solver) for the Boltzmann kinetic equation have revealed anomalous heat and viscous stress transfer effects on the mean free path scale. This study (Aristov et al. 2025) examines nonequilibrium flows featuring novel and diverse nonclassical effects in a monatomic gas. Specifically, it was demonstrated that in these flows, the heat flux vector can oppose the direction predicted by Fourier's law, enabling anomalous heat transfer from cold to hot regions. This effect can also be noted in some other problems (Roohi, 2026; Venugopal et al., 2019; Myong 2011).

The general problem is as follows. In the classical case, heat transfer is described by Fourier's law and viscous transport by Stokes' law. The conditions required for the validity of these

relations are local equilibrium states. In the nonequilibrium case, however, one can propose nonequilibrium distributions such that, for instance, heat can transfer from a cold zone to a hot one. Nevertheless, it is important to find solutions based on kinetic equations for flows with the aforementioned properties. Earlier, we constructed a set of examples for these situations. For instance, in (Aristov et al. 2025), the classical problem of heat conduction but with nonequilibrium boundary conditions demonstrates the nonclassical character of heat transfer. Note that in some problems with equilibrium boundary conditions, e.g., for Poiseuille flow (Myong 2011) the light anomalous heat transfer near the symmetry line is also observed.

Different flows with nonequilibrium boundary conditions demonstrate anomalous heat transfer. Most of the results are presented in (Aristov et al. 2025): several nonuniform relaxation problems, flows through membranes, and supersonic flows through a grid (Aristov et al. 2021; Aristov 2023 et al.). The last type of flow is especially interesting because it allows us to approach a real experiment and can also be compared with the other numerical simulations.

Solutions for a monatomic gas obtained by means of the direct method for solving the Boltzmann equation, the UFS (Unified Flow Solver) (Kolobov et al. 2008), for 1D and 2D problems (where a supersonic equilibrium flow passing through a grid composed of infinite cylindrical bars with a square cross-section becomes a supersonic nonequilibrium flow) demonstrated anomalous heat transfer with a formula

$$\frac{dT}{dx} q_x > 0 \quad .$$

In the present paper, we consider these problems from several points of view. Namely, we attempt to test the effect under different conditions with the help of DSMC variant (Bondar et al. 2008, Kashkovsky et al., 2025) (calculations for diatomic gases) and in the experimental tests by means of the technique from (Ashkenas 1967; Novopashin et al. 1997; Mohamed et al. 2009).

2 Formulation of problems and initial results of computations

At the initial stage of consideration we compare our previous results on the basis of the direct methods for the Boltzmann equation with DSMC for a monatomic gases. The problem under consideration for 1D and 2D variants have been solved for monatomic gases (Aristov et al. 2021; Aristov et al. 2023). This problem models a supersonic flow passing through a grid composed of infinite cylindrical bars of square cross-section. A supersonic flow (2D case) through a grid is studied. The grid is shown in Fig. 1. The flow is directed from left to right, with its velocity vector

normal to the grid plane. To reduce the computational cost, the solution domain is restricted to a half-period, with symmetry conditions imposed at the upper and lower boundaries. In the left boundary the supersonic equilibrium boundary condition is accepted. When passing through a grid a flow is disturbed and this nonequilibrium flow downstream is a subject of investigation. The comparison with the new calculations by SMILE++ software package (Kashkovsky et al. 2025) based on the earlier methods and schemes (Ivanov et al. 2006) confirm anomalous heat transfer downstream by the grid for a monatomic gas.

A more complex and realistic case for a diatomic gas is studied by the DSMC method using this SMILE++ scheme. The results of calculations are presented below.

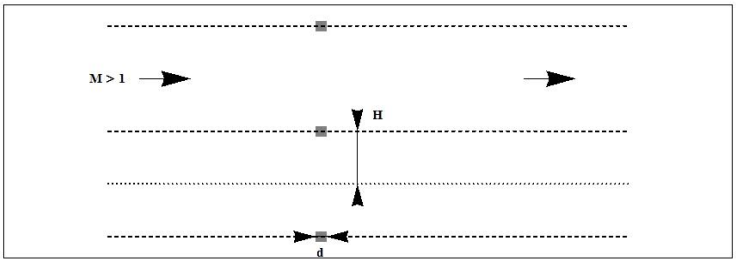

Fig. 1. A scheme of a supersonic flow.

The new flow parameters were as follows: a diatomic gas, nitrogen N_2, was considered; a supersonic equilibrium flow at Mach number M = 4 and Knudsen number Kn = 2 (defined based on the wire diameter of the grid; the Larsen–Borgnakke model (Borgnakke and Larsen 1975) diffusion model (300 K), was adopted for the interaction of gas molecules with the wire).

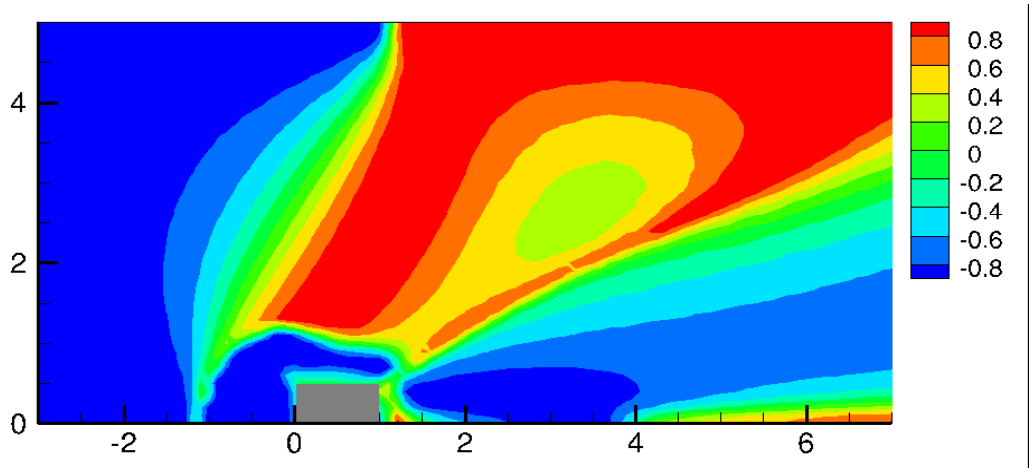

Fig. 2. Field of cos(q, grad(T_{OV})), T_{OV} is overall (translational+rotational) temperature, q *is* heat flux.

The interaction of the gas with this highly permeable grid (permeability of 0.9 or higher) generates a nonequilibrium flow downstream of the grid.

Calculations for a diatomic gas confirm the presence of anomalous heat transfer within this supersonic nonequilibrium region (see Figs. 2–4). Downstream of the grid, the temperature initially rises owing to the interaction between gas molecules and the grid, and then decreases further along the flow. The heat flux remains negative until it reaches zero in the equilibrium region downstream. The anomalous heat transfer is particularly pronounced near the symmetry plane at $y = 0.5$.

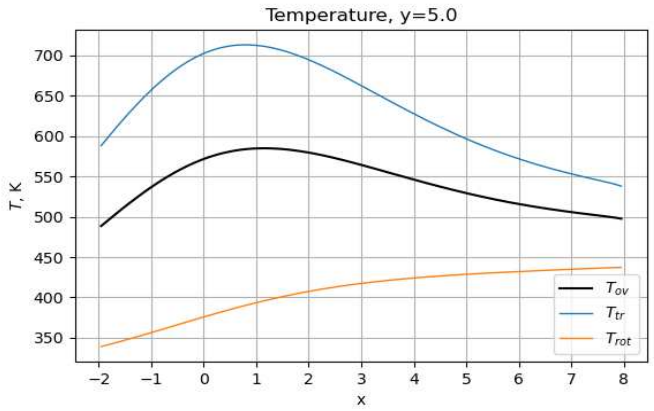

Fig. 3. Profiles of the translational (*tr*), rotational (*rot*) and overall (*ov*) temperatures.

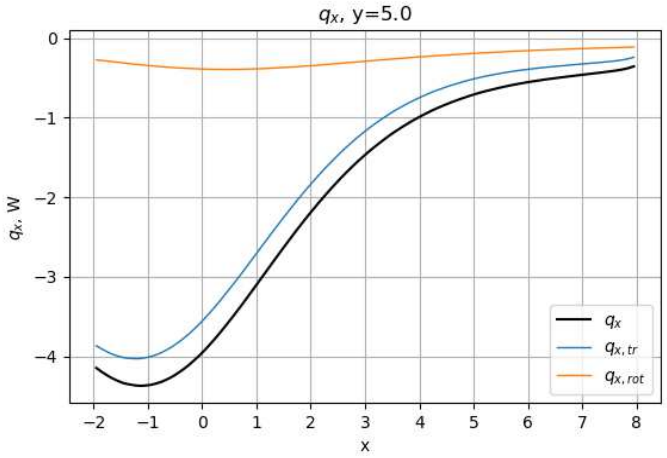

Fig. 4. Profiles of the translational (*x, tr*), rotational (*x, rot*) and overall (*x*) *x*-component of the heat flux.

It can be seen that the translational and overall temperatures exhibit similar behavior — namely, an increase followed by a decrease downstream. The rotational temperature, by contrast, increases monotonically. Notably, the overall temperature gradient and the total heat flux have the same sign near the symmetry axis. The behavior of the rotational quantities is classical. More precisely, the rotational temperature increases and then, as the large distance from the source grows, approaches a constant value; the magnitude of this value can be associated with a certain

"frozen" temperature. In any case Fig. 3 and 4 demonstrate the wide area (for $x > 1$) where the effect of the anomalous heat transfer manifests itself quite clearly.

3 Simulations and experimental results in a search for anomalous effects

We consider the problem of creating nonequilibrium boundary distributions. One approach to solving this problem is to employ a highly permeable grid. An experimental setup designed to produce adequate flows is described. It uses a sonic nozzle that generates a supersonic jet together with a metal grid. The specialized diagnostic equipment includes electron-beam fluorescence (EBF). The first works were e.g. (Ashkenas, 1967; Novopashin et al. 1997; Mohamed et al. 2009). The experiment recorded the nonequilibrium rotational distribution behind the grid. The experimental setup includes a grid with parallel wires (diameter 0.23 mm, spacing 4 mm): Fig. 5. The experimental parameters are given in Table 1.

The parameters not specified in the Table 1 are nozzle pressure of 70 kPa, nozzle diameter of 0.5 mm, nozzle gas temperature of 295K, residual chamber pressure of 1.3 Pa.

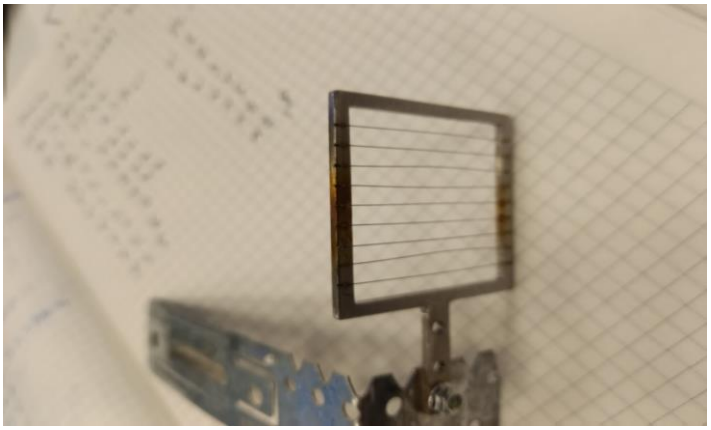

Fig. 5. A grid with parallel wires (diameter 0.23 mm), the distance between which is 4 mm.

Table 1. Parameters of the experiment and the calculations.

№	Distance from the grid to the nozzle	Distance from the measure point to the nozzle	Kn on a grid step (4мм)	Kn On the wire diameter (0.23 mm)
	mm	mm	32	5
	mm	mm	0.65	1

For an adequate comparison with the experiment, some new calculations were performed. The numerical simulation has two stages. The first stage: calculation for the axisymmetric flow from the nozzle (without the grid); the second stage: two calculations of the uniform flow through a grid (variant 1 for distance 20 mm, variant 2 for distance 29 mm), where the flow parameters are taken from the results of the first stage at the grid position. Calculations for the axisymmetric jet flow and a two-dimensional approximation for the near-grid flow confirm the anomalous character of the heat transfer near the symmetry line behind the grid.

Both stages use DSMC with the VHS collision model and the Larsen-Borgnakke energy exchange model. The exact parameters for first stage inlet stream were determined numerically using Ansys Fluent. First stage calculation area is 200x60mm (8713x2614 cells). Second stage parameters: velocity 700 m/s, temperature 10 K, number density 8e20 (variant 1) and 4e20 (variant 2), area 13x2 mm (1300x200 cells).

Figure 6 shows two variants of the second stage, drawn over the results of the first stage.

Calculations for flows for two different Knudsen numbers (Variants 1 and 2) demonstrate qualitatively similar results.

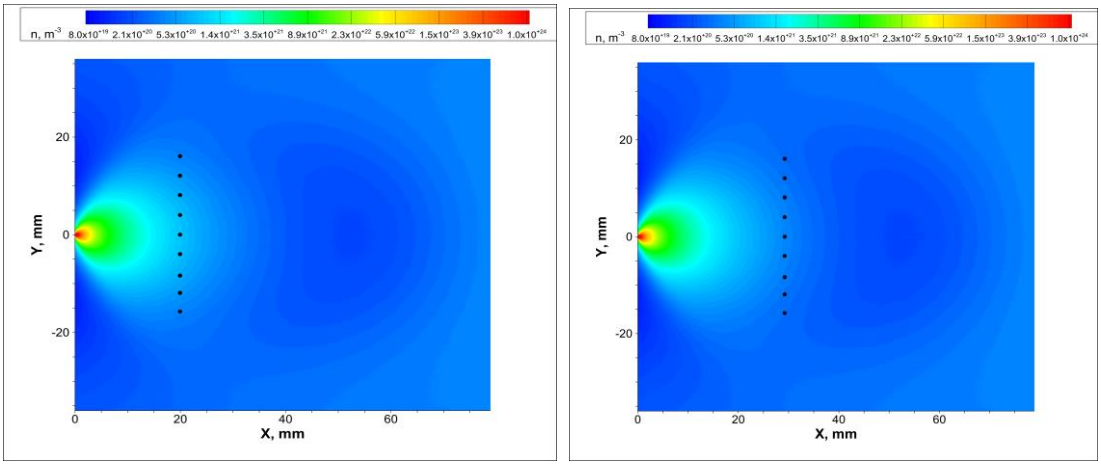

a b

Fig. 6. Fields of density, distance from the grid to the nozzle: d=20 mm (a), d=29 mm (b).

Calculations for the second stage, for both variants, confirm the anomalous character of heat transfer behind the grid, see Fig. 7. Here, a line of symmetry (the line between the wires) is shown on the ordinate axis at a distance of 2 mm. The rotational temperature fields for the two variants are presented in Fig. 8.

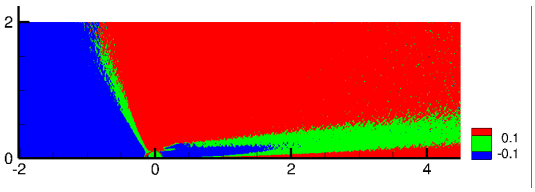

a b

Fig. 7. Stage 2. Field cos(q, grad(T)). 1st variant (a). 2nd variant (b).

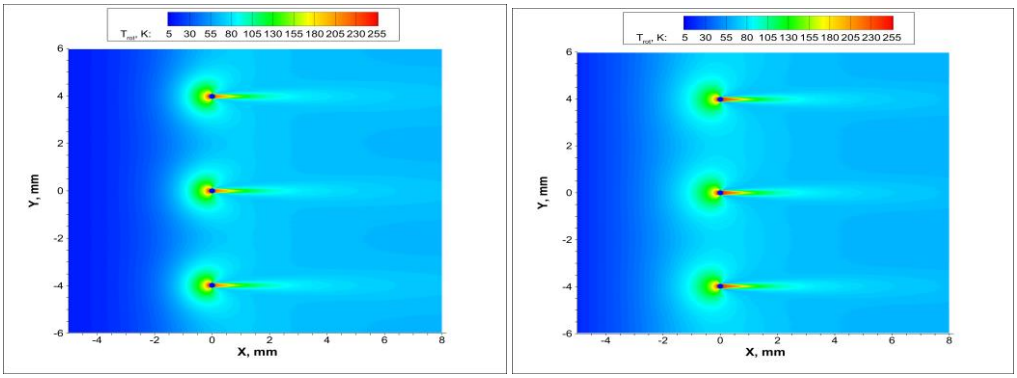

a b

Fig. 8. Fields of rotational temperature behind the grid. Stage 2. 1st variant (a). 2nd variant (b).

The translational temperature is higher than the rotational temperature, and both tend toward the equilibrium value. Profiles of temperature and heat flux along x for the values of y which corresponds the position between wires are shown in Fig. 9 (1st variant) and in Fig. 10 for (2nd variant). It can be seen that, in all cases, anomalous heat transfer occurs: the signs of the overall temperature and the corresponding heat flux component in the downstream region are the same.

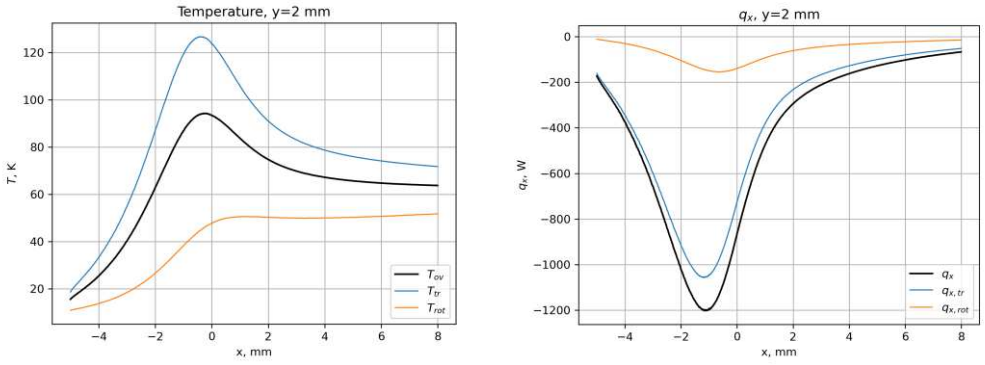

a b

Fig. 9. Temperature (a) and heat flux (b) profiles, 1st variant, $y = 2$ mm.

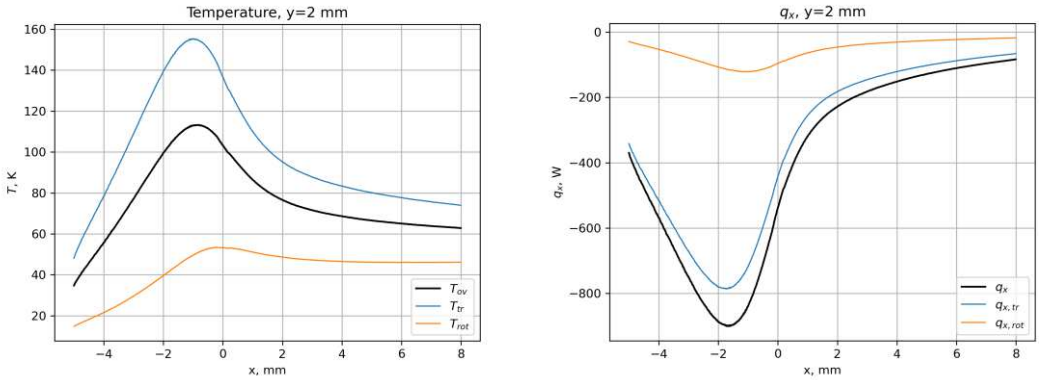

a b

Fig. 10. Temperature (a) and heat flux (b) profiles, 2nd variant, y = 2 mm.

The experimental parameters are as follows: electron beam, pulse energy 20 keV. The experimental results are presented in Figs. 11–15. The equilibrium case demonstrates the linear (in logarithmic scale) population both for a gas at rest and for a gas in a jet, see Fig. 11.

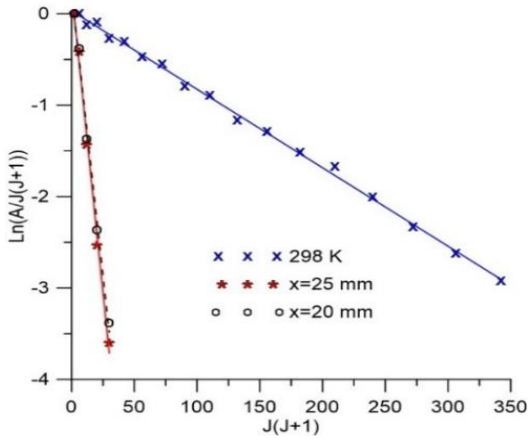

Fig. 11. Population in the gas at rest (left line) and in the jet (right line).

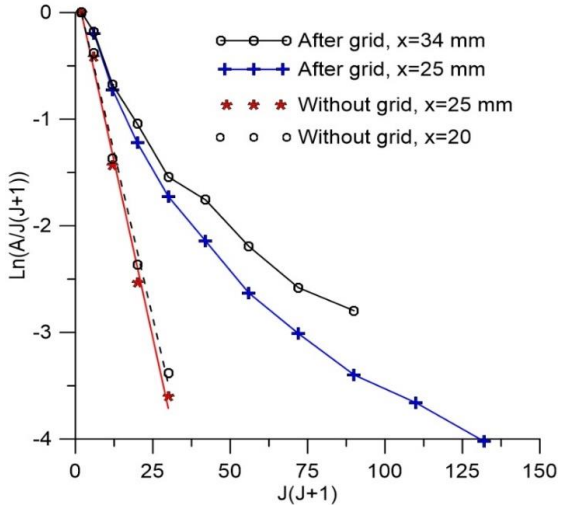

Fig. 12. Rotational population distribution of N_2.

The experimental data for two mentioned variants are given in Fig. 12. For the 1st variant with the grid located at x= 20 mm, the measuring point was located at x= 25 mm, for the second variant with the grid located at x = 29 mm, the measuring point was x = 34 mm. For both cases there is the obvious nonequilibrium rotational population.

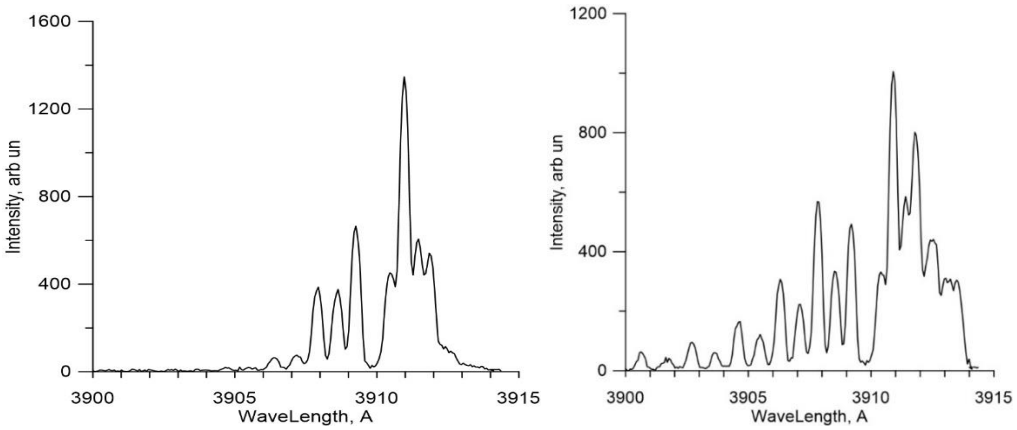

Fig. 13. Nitrogen spectra from the experiment: without the grid (left), and with the grid (right).

In Fig. 13 the nitrogen spectra are shown for the equilibrium case (without the disturbing factor, i.e. the grid) and for the nonequilibrium state (with the grid).

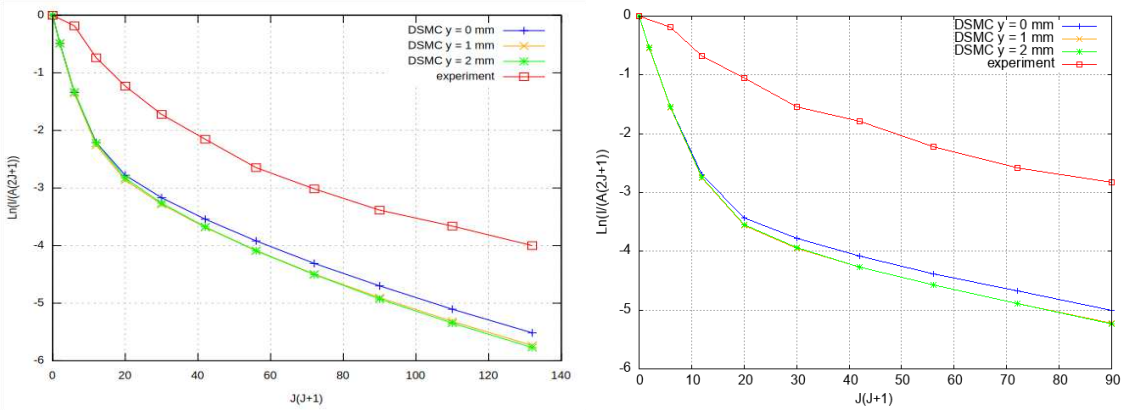

a b

Fig. 14. Comparison of the population of rotational levels in calculations and experiment (x=5 mm behind a grid), after the nozzle x=25 mm (a), after the nozzle x=34 mm (b).

The new calculations correspond qualitatively to this nonequilibrium rotational population for two variants of the experiments and the calculations (see Fig. 14). These results are of interest in their own right, as they confirm the rotational nonequilibrium observed in the experiments. These findings do not directly confirm the anomalous heat transfer, but they indirectly support it owing to the good qualitative agreement with the calculations presented.

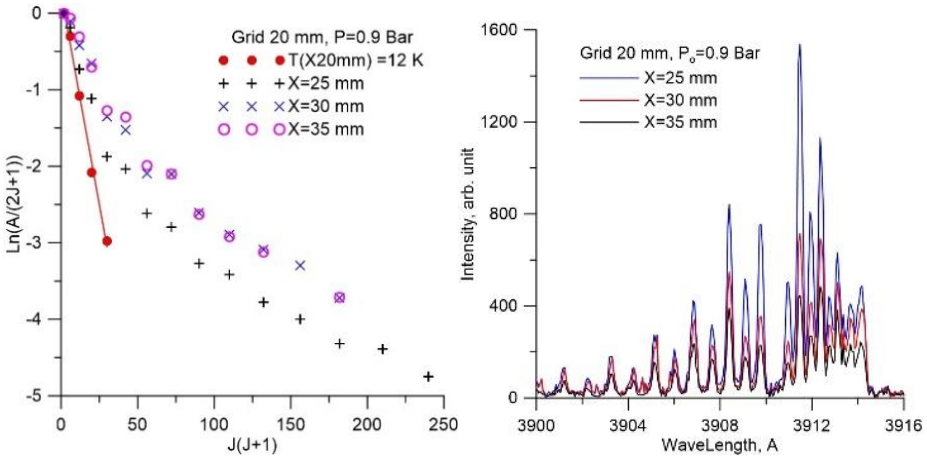

Fig. 15. Population and spectra at different distances behind the grid.

A new series of experiments was carried out. Specifically, the rotational temperature at different points behind the grid can be determined from measurements of the nonequilibrium populations. In Fig. 15 the specific plots for population of the rotational degrees of freedom are shown. Before the grid there is the equilibrium state and therefore we see a straight line. For distances x=5, 10, 15 mm behind the grid the flows are nonequilibrium. The incline the plot is proportional $1/T_R$. This temperature increases downstream and tends to a certain limit, this corresponds to the calculations. In Fig. 15 spectra in the appropriate points behind the grid are also depicted, one can the nonequilibrium character of these plots.

Several important questions arise. In particular, we obtained a nonequilibrium rotational distribution at a point behind the grid, but we are more interested in the translational nonequilibrium distribution. These states can only be inferred indirectly. Nevertheless, the qualitatively similar populations and the downstream increase in rotational temperature found in the calculations support the validity of our conclusion. Strictly speaking, we should construct the nonequilibrium distribution function, but this is a matter for future, more precise experiments.

4 Conclusions and discussion

We have shown that for a supersonic rarefied gas flow through a grid, a nonequlibrium distribution with anomalous heat transfer properties exists downstream. Calculations for monatomic and diatomic gases and the first experiments indirectly confirm this effect. For the first time, the nonequilibrium rotational temperature behind the grid has been measured.

Possible areas of application of this effect can be discussed, in particular, the cooling of micro-objects. It is known that cooling is an issue in microelectronics. We propose a first possible application for this purpose, based on the described anomalous heat transfer effect. An element

maintained at a constant temperature is supported in a flow, where normal heat exchange with the equilibrium flow occurs owing to wall contact with the flow. This heat is then transferred downstream. The cold equilibrium state is located near this element. We consider a nonequilibrium flow (for example behind a grid) from left to right. In the left there is a nonequilibrium distribution at temperature T_{noneq} in the right there is an equilibrium distribution at temperature T_{eq}.. The aim is to maintain the temperature T_c of the sample. The anomalous heat transfer helps it as the heat flux directs from the cold to the hot region. This phenomenon could serve as the basis for the development of new technological models and devices. Incidentally, this could also serve as a possible experimental setup for testing this effect.

Some of these interesting issues could be explored in the future; they might serve as the subject of a separate scholarly study.

Declarations

Conflict of interest The authors declare no competing interests.

Contributions

V.A.: Conceptualization, Methodology, Investigation, Analysis of Results, Writing

T.M.: Methodology, Calculations, Investigation, Writing

S.N.: Methodology, Experiments, Investigations, Analysis of Results

References

Akhlaghi H, Roohi E, Stefanov S (2023) A comprehensive review on micro- and nano-scale gas flow effects: slip-jump phenomena, Knudsen paradox, thermally-driven flows, and Knudsen pumps. Physics Reports 997: 1-60. doi:10.1016/ j.physrep.2022.10.004

Schafer BC, Kim J, Sharipov F, Hwang G-S, Vlassak JJ, Keith DW (2025) Photophoretic flight of perforated structuresinnear-space conditions. Nature 644: 362-369 https://doi.org/10.1038/s41586-025-09281-8.

Aristov VV, Zabelok SA, Frolova AA (2025) Nonclassical transport in nonequilibrium rarefied gas flows. Uspekhi Fizicheskikh Nauk, 195: 276-293. https://doi.org/10.3367/UFNr.2024.08.039730.

Roohi E. What does anti-Fourier heat-flux agreement validate? Observability of the fourth-order closure state in a rarefied lid-driven cavity. arXiv:2609.27892v1 [physics.flu-dyn] 21 Aug 2026

Venugopal V, Praturi DS, Girimaji SS (2019) Non-equilibrium thermal transport and entropy analyses in rarefied cavity flows. J Fluid Mech 864: 995–1025 doi:10.1017/jfm.2018.1028

Myong RS (2011) A full analytical solution for the force-driven compressible Poiseuille gas flow based on a nonlinear coupled constitutive relation Phys Fluids. 23: 012002. https://doi.org/10.1063/1.3540671

Aristov VV, Voronich IV, Zabelok SA (2021) Nonequilibrium nonclassical phenomena in regions with membrane boundaries Phys Fluids. 33 : 012009 https://doi.org/10.1063/5.0036089

Aristov VV, Voronich IV, Zabelok SA (2023) Study of Nonclassical Transport by Applying Numerical Methods for Solving the Boltzmann Equation Comp. Math. Math. Phys. 2023 63 (12): 2306-2314 https://doi.org/10.1134/S0965542523120047

Kolobov VI, Arslanbekov RR, Aristov VV, Frolova AA, Zabelok SA (2007) Unified solver for rarefied and continuum flows with adaptive mesh and algorithm refinement J. Comp. Phys. 223(2):589-608 DOI:10.1016/j.jcp.2006.09.021

Ivanov M, Kashkovsky A, Gimelshein S, Markelov G, Alexeenko A, Bondar Te, Zhukova G, Nikiforov S, Vaschenkov P (2006) SMILE system for 2D/3D DSMC computations, *Proc. 25th Int. Symp. on Rarefied Gas Dynamics*, Saint Petersburg. 21–28.

Kashkovsky AV, Vashchenkov PV, Shevyrin AA *et al.* (2025) Smile Family of Software Systems for the Direct Monte Carlo Simulations of Rarefied Gas Flows. *J Eng Phys Thermophy* 98: 1872–1897 https://doi.org/10.1007/s10891-026-03266-8

Borgnakke C, Larsen PS (1975) Statistical collision model for Monte Carlo simulation of polyatomic gas mixture, J Comput Phys, 18:405-420. https://doi.org/10.1016/0021-9991(75)90094-7

Ashkenas H (1967) Rotational temperature measurements in electron beam excited nitrogen. Phys Fluids. 10(12): 2509. http://dx.doi.org/10.1063/1.1762070

Novopashin S, Dankert C, Lehmköster K, Mohamed A, Pot T (1997) Rotational Temperatures of N_2-molecules Reflected from a Wall (1997) Rarefied Gas Dynamics, Proceedings of the 20th International Symposium, 19-23 August 1996, Beijing/China, Ed. Ching Shen, Peking University Press, Beijing, China, 428-433.

Mohamed AK, Bonnet J, Larigaldie S, Pot T, Soutadé J et al. (2009) Electron Beam Fluorescence in Hypersonic Facilities. Aerospace Lab, 1: 1-9. ⟨hal-01180669 https://hal.science/hal-01180669v1